Estimating Hail Size using Polarimetric Radar

Angela Rowe

National Weather Center Research Experiences for Undergraduates, and Millersville University, Millersville, PA

Pamela L. Heinselman[1] and Terry Schuur[1]

Cooperative Institute for Mesoscale Meteorological Studies, University of Oklahoma, Norman, Oklahoma

1. Also affiliated with NOAA/National Severe Storms Laboratory, Norman, Oklahoma

Corresponding author address: Angela Rowe, 13233 Rowe Rd., Smithsburg, MD, 21783
Email: akrowe@marauder.millersville.edu

ABSTRACT

This study investigates the use of polarimetric variables for estimating hail size. Archived data from the KOUN polarimetric radar in Norman, Oklahoma are obtained for three hail-producing events: 24 May 2004, 29 May 2004, and 2 June 2004. A total of 45 hail reports are used for analysis, including hail sizes ranging from 0.75" to 4.25". Horizontal and vertical structures of reflectivity (Z_H), differential reflectivity (Z_{DR}), and correlation coefficient (ρ_{HV}) associated with these reports are examined using Interactive Data Language (IDL) programs. Comparison of these images allow for the hail to be categorized into two groups based on Z_{DR} and ρ_{HV} signatures: category 1: hail less than 1.75" in diameter and hail 1.75" or higher in diameter. RHI images reveal differences in the vertical structures of these categories; extended columns of low Z_{DR} and ρ_{HV} are observed for the larger hail. Also, vertical profiles, produced for each report, show a more substantial decrease in ρ_{HV} below the melting layer for hail 1.75" or larger. Box-and-whisker plots and discriminant analysis are then used to determine the ability of Z_{DR} and ρ_{HV} to distinguish between the two categories. Although Z_{DR} appeared promising for estimating hail size, the discriminant analysis revealed that ρ_{HV} is the best variable to discriminate between the categories.

1. Introduction

The National Weather Service (NWS) completed the installation of the current national network of Weather-Surveillance Radar-1988 Dopplers (WSR-88Ds) in 1997 (Doviak et al. 2000). A few years later, the National Severe Storms Laboratory acquired a WSR-88D (KOUN) specifically for research purposes (Doviak et al. 2000). This radar was modified to test dual-polarization techniques, in which a pulse is transmitted simultaneously in the horizontal and vertical. An upgrade of the entire WSR-88D national network to include dual-polarimetric capabilities is expected by about 2010. This upgrade is motivated by results of an experiment that was conducted from March 2002 to June 2003 called the Joint Polarization Experiment (JPOLE). This experiment was designed to evaluate the design and data quality of the KOUN polarimetric radar, as well as to demonstrate the application of its products for operational purposes (Schuur et al. 2003a). Data was collected from KOUN for 98 weather events, and evaluation of this data led to significant improvements in rainfall estimation, separation of meteorological echoes from nonmeteorological echoes, and hail classification (Ryzhkov et al. 2003, Schuur et al. 2003b).

The detection of hail and its size has been a long-standing goal of radar meteorologists (e.g. Straka et al. 2000). Currently, the probability of hail within a storm is determined operationally by the WSR-88D Hail Detection Algorithm (HDA). This empirically derived probability is based primarily on the vertical structure of reflectivity data collected at horizontal polarization (Witt et al. 1998). Through the simultaneous

horizontal and vertical transmission of the pulse, dual-polarization radar provides additional information regarding the shape, size, and distribution of the hydrometeors. These properties are determined by interpreting polarimetric variables such as differential reflectivity factor (Z_{DR}), correlation coefficient (ρ_{hv}), and specific differential phase (K_{DP}) (e.g., Zrnić and Ryzhkov 1999; Straka et al. 2000). Using polarimetric variables, the Hydrometeor Classification Algorithm (HCA) pinpoints the location of different hydrometeor types in a storm. In terms of overall accuracy and skill, HCA outperforms the current HDA (Schuur et al. 2003b). HCA is more effective for detecting hail because it determines the actual location of the hail, whereas HDA only provides a probability of hail within a storm.

Dual-polarization radar not only supplies information for hydrometeor classification, but may also prove useful for gauging hail size within the storm. Past research indicates relationships between the polarimetric variables (primarily Z_{DR} and ρ_{hv}) that allow for hail size to be categorized (e.g., Balakrishnan and Zrnić 1990). Investigating the relation of polarimetric variables to hail size can be beneficial in improving warnings for hail producing storms, understanding the physical processes that lead to hail formation, and determining possible precursive signatures associated with hail formation and growth.

The goal of this study is to investigate the use of polarimetric variables to estimate maximum hail size within a storm. This will be achieved through interpretation of polarimetric KOUN radar data during three hail-producing events. These variables and their application for gauging hail size are discussed further in section 2. The methods

used to analyze the polarimetric data are presented in section 3, and section 4 reveals the results. The summary and concluding remarks are provided in section 5.

2. Polarimetric variables used for investigating hail size

Previous studies indicate that the variables of interest for gauging hail size include reflectivity at horizontal polarization (Z_H), Z_{DR}, ρ_{hv}, and K_{DP} (e.g., Balakrishnan and Zrnić 1990; Zrnić et al. 1993; Straka et al. 2000). Reflectivity at horizontal polarization is proportional to the cross section of a hydrometeor and is weighted heavily by hydrometeors of largest diameter within the volume. Therefore, in regions of hail, Z_H generally increases with respect to rain regions (Aydin et al. 1986). Combined with other polarimetric variables, Z_H may be useful for estimating the maximum hail size within the storm.

Differential reflectivity is the ratio of the returned power in the horizontal (Z_H) to the returned power in the vertical (Z_V):

$$Z_{DR} = 10 \log (Z_H/Z_V) \quad (1)$$

Because Z_{DR} is a logarithmic function, the sign of Z_{DR} provides information concerning the orientation of the hydrometeors within the volume. Positive values of Z_{DR} represent horizontally oriented hydrometeors (i.e., rain), values near 0 indicate either spherical hydrometeors (i.e., hail) or tumbling hail, and values less than 0 indicate vertically oriented hydrometeors (i.e., graupel or hail with a conical shape). Aydin et al. (1986)

introduced a new hail signal (H_{DR}) that accounted for the negative correlation between Z_{DR} and Z_H. Results from this paper indicated that for their two investigated hail-producing storms, H_{DR} increased as hail size increased.

The correlation coefficient is a measure of decorrelation of hydrometeors within a volume. Meteorological scatterers typically have ρ_{hv} values higher than 0.7; for rain, it's higher than 0.95, and for hail, generally lower than 0.95. Because correlation coefficient decreases with increasing size of hailstones in both a mixture of hail and rain and within a mixture of hail sizes, Balakrishnan and Zrnić (1990) hypothesized that ρ_{hv} can be used to infer maximum hail diameters.

The specific differential phase is a range derivative of the differential phase shift. The presence of hydrometeors within a volume causes the electromagnetic waves to propagate at different speeds in the horizontal and vertical directions, producing a noticeable phase shift. This allows discrimination of hydrometeors based on their shape and number concentration. Values of K_{DP} range from -1 ° km^{-1} to 6 ° km^{-1}, where higher values indicate higher rain rates. Unlike Z_H, K_{DP} is fairly insensitive to hail (i.e., K_{DP} ~0), allowing for a more accurate rain rate to be determined. The specific differential phase may also be useful for looking at processes within a hail-producing storm. Throughout a study of two hail-producing events, Balakrishnan and Zrnić (1990) observed an increase in K_{DP} from the top of the melting layer to the ground for the event producing larger hail. This indicated that melting was the dominant process, as opposed to breakup and

coalescence. The possible implications for using K_{DP} to gauge hail size will be discussed in later sections.

Balakrishnan and Zrnić (1990) attempted to categorize hail size by also investigating the effects of various hail models on Z_{DR} and ρ_{hv}. Throughout their investigation, the larger hail produced negative Z_{DR}. Results of Balakrishnan and Zrnić (1990) also revealed a significant difference in Z_{DR} and ρ_{hv} signatures for hail larger than 5 cm (1.97") compared to signatures for hail smaller than 5 cm. Specifically, Z_{DR} of dry, oblate hailstones became negative at a diameter of 5 cm, and a significant decrease in ρ_{hv} occurred for wet, oblate hail when the size of the hailstone reached 5 cm.

In this study, Z_H, Z_{DR}, and ρ_{hv} are the primary variables investigated to estimate hail size. Three hail-producing events are used to obtain a larger data set of hail reports for comparison with the two cases observed by Balakrishnan and Zrnić (1990). Details about these events and the methods for investigating the polarimetric data are discussed further in the next section.

3. Methods for displaying polarimetric data

In this study, KOUN polarimetric data are investigated for three hail-producing events in Oklahoma, including 24 May 2004, 29 May 2004, and 2 June 2004. On 24 May 2004, KOUN detected a line of supercells extending from Harmon County to

Washita County, moving East-Northeast. During this event (2145 UTC 24 May 2004−0535 UTC 25 May 2004), the NWS in Norman, Oklahoma received 60 hail reports ranging in size from 0.75" to 2.75" in diameter. On 29 May 2004, a cyclic supercell was observed by KOUN first in Roger Mills County at about 2100 UTC. This long-lived supercell moved eastward toward Oklahoma County, producing hail as large as 4.25". By 0554 UTC 30 May 2004, there were 38 reports of hail throughout western and central Oklahoma. Finally, on 2 June 2004, a squall line, producing high wind and hail, moved south from Oklahoma County towards the Texas border. During this event (1710 UTC 2 June 2004−0120 UTC 3 June 2004), there were 61 hail reports ranging from 0.75" to 1.75".

Prior to analysis, these storm reports are verified and the polarimetric data are corrected for errors and bias. The archived data from these three days are displayed using the Warning Decision Support System-Integrated Information (WDSS-II). Hail reports are verified by comparing their location to 0.5° elevation Z_H, Z_{DR}, and ρ_{hv} images for the time most closely associated with the report. Then, owing to radar limitations, the hail reports farther than 150 km away from the radar were removed from the data set. Following these steps, the remaining hail reports are reduced from 149 to 45.

Next, the data are corrected for errors and bias. The KOUN reflectivity data are compared to reflectivity data from a nearby WSR-88D (KTLX), located 20 km NE of KOUN. In comparison, reflectivity values on 24 May 2004 were 3 dBZ lower, whereas the reflectivity values were 3 dBZ higher on 29 May 2004 and 2 June 2004. The

correlation coefficient also is adjusted for the different cases because it is noticeably biased for signal-to-noise ratios (SNR) less than 20 dB (Schuur et al. 2003b). The SNR is a function of reflectivity, range, and the radar constant. Using an Interactive Data Language (IDL) program, the ρ_{hv} values are plotted against the SNR. For each report, the value of the radar constant used for computing SNR is adjusted so that the plot is flat (i.e., there is no dependence of ρ_{hv} on SNR for SNR > 5dB) (Schuur et al. 2003b). The values of Z_{DR} are reasonable and do not have to be corrected.

After the polarimetric variables are corrected, IDL programs are used to display the data in a variety of ways. First, the data are viewed by creating Plan Position Indicator (PPI) images. For each hail report, the 0.5 elevation Z_H, Z_{DR}, ρ_{hv} data, and hydrometeor classification output are displayed to discern polarimetric signatures associated with the location of the report. Second, scatterplots of Z_H versus Z_{DR}, Z_H versus ρ_{hv}, and Z_{DR} versus ρ_{hv} are produced for each hail report to determine relationships between the variables for the various hail sizes. Third, Range Height Indicator (RHI) images are created along the azimuth and range of the hail signature selected from the PPI. Values of Z_H, Z_{DR}, ρ_{hv}, and K_{DP} are plotted versus height to examine the vertical structure of hail within a storm. Fourth, vertical profiles, similar to those produced for the Balakrishnan and Zrnić study (1990), are created for a given azimuth and distance from the radar. These are beneficial for obtaining specific values of the variables for the different heights in the storm, which provides a more detailed comparison of values of the different hail sizes.

These techniques are useful for assessing the relation of polarimetric data to hail size both quantitatively and qualitatively. Investigation of the signatures and values associated with the different sizes provides significant results regarding the use of polarimetric variables for estimating the maximum hail size within a storm. These results are presented in the following section.

4. Relation of Polarimetric data to hail size

Using the techniques described above, the hail reports are grouped based on their Z_H, Z_{DR}, and ρ_{hv} signatures and values. The hail sizes with similar signatures are grouped together, and the division of the data into another group occurs at the size at which the signatures begin to differ. This process results in two categories: 1) hail smaller than 1.75" and 2) hail 1.75" or larger. Category 1 included 7 reports of 0.75" hail, 6 reports of 0.88" hail, 13 reports of 1.00", 2 reports of 1.25", and 1 report of 1.50", whereas Category 2 included 9 reports of 1.75" hail, 2 reports of 2.00" hail, 1 report of 2.50" hail, 4 reports of 2.75" hail, and 1 report of 4.25" hail. The polarimetric characteristics of each category are described in detail below.

The PPI images provide a large scale view of the hail-producing events for a broad comparison of polarimetric variables between the two different categories. Figures 1a−f display the Z_H, $Z_{DR,}$ and ρ_{hv} PPI images that represent the characteristics of at least 70% of all the images in each hail size category. The 1.00" hail report (Figs. 1a, c, and e)

occurred at 2236 UTC on 2 June 2004, whereas the 1.75" report (Figs. 2b, d, and f) occurred at 0200 UTC on 24 May 2004. Although the reflectivity fields for both reports are similar (c.f. Figs. 1a, b), there is a noticeable difference in the Z_{DR} and ρ_{hv} signatures. The Z_{DR} field associated with the 1.00" hail (category 1) has a broad area of values between 1.5 and 3 dB, with a minimum of approximately 1 dB (Fig. 1c). The larger hail is associated with a negative Z_{DR} minimum within a large area of values less than 1dB (Fig. 1d). Negative Z_{DR} values, which are typically associated with hail 1.75" or larger in diameter, are rarely observed for the smaller hail. Another difference between the two sizes is seen in the ρ_{hv} PPI images. Category 1 sizes generally have broad areas of ρ_{hv} equal 0.95 or higher (i.e., Fig. 1e), whereas the larger hail in category 2 have large areas of ρ_{hv} lower than 0.95 (i.e., Fig. 1f). Although the two reports are located at different distances from the radar, the signatures observed are representative of the majority of reports regardless of their range. The scatterplots produced from these PPI images emphasize the concentration of lower Z_{DR} and ρ_{hv} values for the 1.75" hail compared to the 1.00" hail (Fig. 2).

The RHI images reveal differences in the vertical structures of the 1.00" and 1.75" hail. Within the storm core, the lowest values of ρ_{hv} and Z_{DR} in the cloud for the larger hail extend to a higher height within the cloud than those for the smaller hail. These extended columns for 1.75" hail show that hail exists farther aloft indicating a stronger updraft and allowing for the hailstones to grow larger in size before falling to the ground. Like the previous PPIs and scatterplots, the RHIs show that at the base of the cloud, Z_{DR} and ρ_{hv} values for the 1.75" hail are lower than those for 1.00" (Figs. 3c−f).

Another interesting feature is the overhang of high reflectivity values offset from the main core seen in the category 2 RHI image only (Fig. 3b). It has been speculated that this overhang could be a possible source of embryos that lead to production of large hail. In another study involving polarimetric variables and hail size, Hubbert et al. (1998) inferred that melting graupel produced the reflectivity overhang for their case, by forming a low-level curtain of drizzle. They believed this to be the embryo source for the large hail. We speculate that the same processes occurred in the 24 May 2004 storm.

Next, vertical profiles are produced from the RHI images that supplied values of Z_{DR} and ρ_{hv} useful for comparing ranges of values for each category (Fig. 4). Maximum values of reflectivity near the cloud base are similar for both hail sizes (c.f. Figs. 4a, b). This lack of difference in reflectivity demonstrates the importance of using Z_{DR} and ρ_{hv} for discriminating between different hail sizes (Fig. 4). The vertical profiles of the variables were similar to those produced for the Balakrishnan and Zrnić (1990) cases. For example, the Z_{DR} profile of the larger hail from my study remains around 0 dB throughout most of the column, and increases below the melting layer for the smaller hail. This profile was also observed in the previous study by Balakrishnan and Zrnić (1990). The profile for ρ_{hv} also coincides with the previous study in that it decreases dramatically below the melting layer for the larger hail, but decreases less for the smaller hail. An extreme case of this drastic decrease in ρ_{hv} is observed in the vertical profile of the 4.25" hail report (Fig. 5), where ρ_{hv} decreases to a value below 0.8. For this profile, higher values of Z_{DR} below the melting layer are observed, along with a decrease in K_{DP}.

This suggests that there is large, water-coated hail with a low mixture with rain. Finally, investigation of the K_{DP} profiles for the two categories reveals a noticeable difference between the two sizes. However, no significant similarities in K_{DP} are observed between the various sizes of each category (Fig. 4).

Values of ρ_{hv} and Z_{DR} are also compared at the lowest heights using these vertical profiles. At the cloud base, the 1.00" hail has a ρ_{hv} value of 0.94 (Fig. 4a), whereas the 1.75" hail has a ρ_{hv} value of 0.89 (Fig. 4b). The difference in Z_{DR} is also shown through these profiles, with a Z_{DR} of 1.26 dB for the 1.00" hail (Fig. 4a) and -0.08 dB for the 1.75" hail (Fig. 4b).

To confirm the apparent differences of near-surface values of Z_{DR} and ρ_{hv} between the two categories, the distributions of these variables were examined by using box-and-whisker plots (Fig. 6). From the ρ_{hv} boxplot, it appears that the two categories are distinguishable by a ρ_{hv} threshold of 0.91 (Fig. 6a). However, it is more difficult to establish a Z_{DR} threshold that distinguishes categories because there is an area of overlapping values (Fig. 6b). Thus, it is worth investigating further whether ρ_{hv} alone is sufficient for discriminating between category 1 and category 2, or if it is more beneficial to combine ρ_{hv} with Z_{DR}.

To investigate the relationship between these variables, the data are analyzed using discriminant analysis. This is a statistical method used to determine which variables are best for discriminating between different groups. A quadratic discriminant function is

developed for ρ_{hv} versus Z_H (Fig. 7a) and ρ_{hv} versus Z_{DR} (Fig. 7b), which provides details about the division line for the two categories. The purpose of this function is to allow future observations to accurately be classified into the different groups (Wilks 1995). For both plots, most of the reports for category 1 are grouped together to the left of the line, and the category 2 reports are generally grouped together on the other side. This shows that, overall, the discriminant function serves as the dividing line between the two categories.

In order to determine which relationship between variables is more useful for discriminating between the categories, a 2x2 contingency table has been produced for both plots to determine the probability of detection and false alarm rate for each category. For the ρ_{hv} versus Z_H plot, the probability of detection of category 1 hail is 81%, and the probability of detection of category 2 hail is 79%. The false alarm rates for category 1 hail and category 2 hail are 19%, and 21%, respectively. For the ρ_{hv} versus Z_{DR} plot, the probability of detection of category 1 hail is 78% and the probability of detection of category 2 hail is 77%. The false alarm rates for category 1 hail and category 2 hail are 23% and 22%, respectively.

By comparing the probabilities for both plots, we conclude that using Z_{DR}, instead of Z_H, with ρ_{hv} does not improve the probability of detection. Probabilities of detection for the Z_{DR} / ρ_{hv} plot are actually even slightly lower than those for the Z_H / ρ_{hv} plot. This difference can be attributed to the data points located close to the discriminant line, where the category 2 hailstones located in this region are 1.75", but have high Z_{DR} values, and

the category 1 hailstones are the largest of that category. Considering the similarity of these sizes, we infer that the category 2 hail have a water coating and are more oblate, resulting in characteristics similar to category 1. This result indicates that additional research of hail-producing storms is required to improve the understanding of the affects of the water content and shape on the polarimetric variables. This study reveals that of the polarimetric variables investigated (Z_H, Z_{DR}, ρ_{hv}, and K_{DP}), the correlation coefficient most accurately estimates the maximum hail size within a storm.

5. Summary and Concluding Remarks

This study investigates the use of polarimetric variables (Z_H, Z_{DR}, ρ_{hv}, and K_{DP}) for estimating hail size. A total of 45 hail reports from 3 hail-producing storms that occurred on 24 May 2004, 29 May 2004, and 2 June 2004 are used for this study. Horizontal and vertical signatures of polarimetric data associated with these hail reports are examined for a variety of hail sizes, ranging from 0.75" to 4.25". Noticeable differences in Z_{DR} and ρ_{hv} signatures occur when hail sizes reach 1.75" in diameter, resulting in the separation of events into two categories. This finding corresponds well with the results from Balakrishnan and Zrnić (1990) who showed that Z_{DR} and ρ_{hv} signatures change when the hail reaches a size of 5 cm (1.97"). Based on the current study's results, hail size may be estimated as smaller than 1.75" in diameter or 1.75" and larger in diameter using polarimetric data.

Although Z_{DR} appeared promising for estimating hail size, discriminant analysis of the data reveals that ρ_{hv} distinguishes hail sizes best. Indeed, the probability of detection of each category using ρ_{hv} does not improve when compared with Z_{DR} instead of Z_H. This further proves that ρ_{hv} is more useful than Z_{DR} for accurately categorizing the hail.

The discriminant functions discussed in this study seem promising for automated estimation of hail size based primarily on ρ_{hv}. The PPIs and RHIs are also valuable for discriminating hail size. Negative Z_{DR} values associated with broad areas of ρ_{hv} lower than 0.95 on PPI images are a good indicator of hail 1.75" or larger. In addition, observing deep vertical columns of lower Z_{DR} and ρ_{hv} in the RHI images helps to categorize the hail as 1.75" or larger with even more confidence. These PPI and RHI signatures, combined with results associated with the discriminant functions, will provide forecasters with the information needed to alert the public of potentially dangerous situations associated with large hail.

Acknowledgements: The IDL programs used in this study were written by the Weather Radar Research and Development branch. We are grateful to the NWS in Norman, OK for providing a complete list of the storm reports. We would also to like to thank Daphne Zaras, director of the National Weather Center Research Experience for Undergraduates (NWC REU) program. The NWC REU was supported by the National Science Foundation under Grant No. 0097651.

References

Aydin, K., T. A. Seliga, and V. Balaji, 1986: Remote sensing of hail with a dual linear polarization radar. *J. Climate Appl. Meteor.,* **25,** 1475−1484.

Balakrishnan, N., and D. S. Zrnić, 1990: Use of polarization to characterize precipitation and discriminate large hail. *J. Atmos. Sci.,* **47,** 1525−1540.

Doviak, R. J., V. Bringi, A. Ryzhkov, A. Zahrai, and D. Zrnić, 2000: Considerations for polarimetric upgrades to operational WSR-88D radars. *J. Atmos. Oceanic Technol.,* **17,** 257−278.

Hubbert, J., V. N. Bringi, L. D. Carey, and S. Bolen, 1998: CSU-CHILL polarimetric radar measurements from a severe hail storm in Eastern Colorado. *J. Appl. Meteor.,* **37,** 749−775.

Ryzhkov, A., S. Giangrand, and T. Schuur, 2003: Rainfall measurements with the polarimetric WSR-88D radar, Report of the National Severe Storms Laboratory, Norman, OK, 98 pp. [Available from the NSSL, 1313 Halley Circle, Norman, OK 73069]

Schuur, T., P. Heinselman, K. Scharfenberg, A. Ryzhkov, D. Zrnić, V. Melnikov, and J. Krause, 2003a: Overview of the Joint Polarization Experiment (JPOLE), Report of the National Severe Storms Laboratory, Norman, OK, 39 pp. [Available from the NSSL, 1313 Halley Circle, Norman, OK 73069]

−−−−, A. Ryzhkov, P. Heinselman, D. Zrnić, D. Burgess, and K. Scharfenberg, 2003b: Observations and classification of echoes with the Polarimetric WSR-88D Radar,

Report of the National Severe Storms Laboratory, Norman, OK, 46 pp. [Available from the NSSL, 1313 Halley Circle, Norman, OK 73069]

Straka, J. M., D. S. Zrnić, and A. V. Ryzhkov, 2000: Bulk hydrometeor classification and quantification using polarimetric radar data: synthesis of relations. *J. Appl. Meteor.,* **39,** 1341−1372.

Wilks, D.S., 1995: *Statistical Methods in the Atmospheric Sciences*. Academic Press, 408−419.

Witt, A., M. D. Eilts, G. J. Stumpf, J. T. Johnson, E. D. Mitchell, and K. W. Thomas, 1998: An enhanced hail detection algorithm for the WSR-88D. *Wea. Forecasting*, **13**, 286−303

Zrnić, D.S. and A. V. Ryzhkov, 1999: Polarimetry for weather surveillance radars. *Bull. Amer. Meteor. Soc.,* **80,** 389−406.

−−−−, V. N. Bringi, N. Balakrishnan, K. Aydin, V. Chandrasekar, and J. Hubbert, 1993: Polarimetric measurements in a severe hailstorm. *Mon. Wea. Rev*., **121**, 2223−2238.

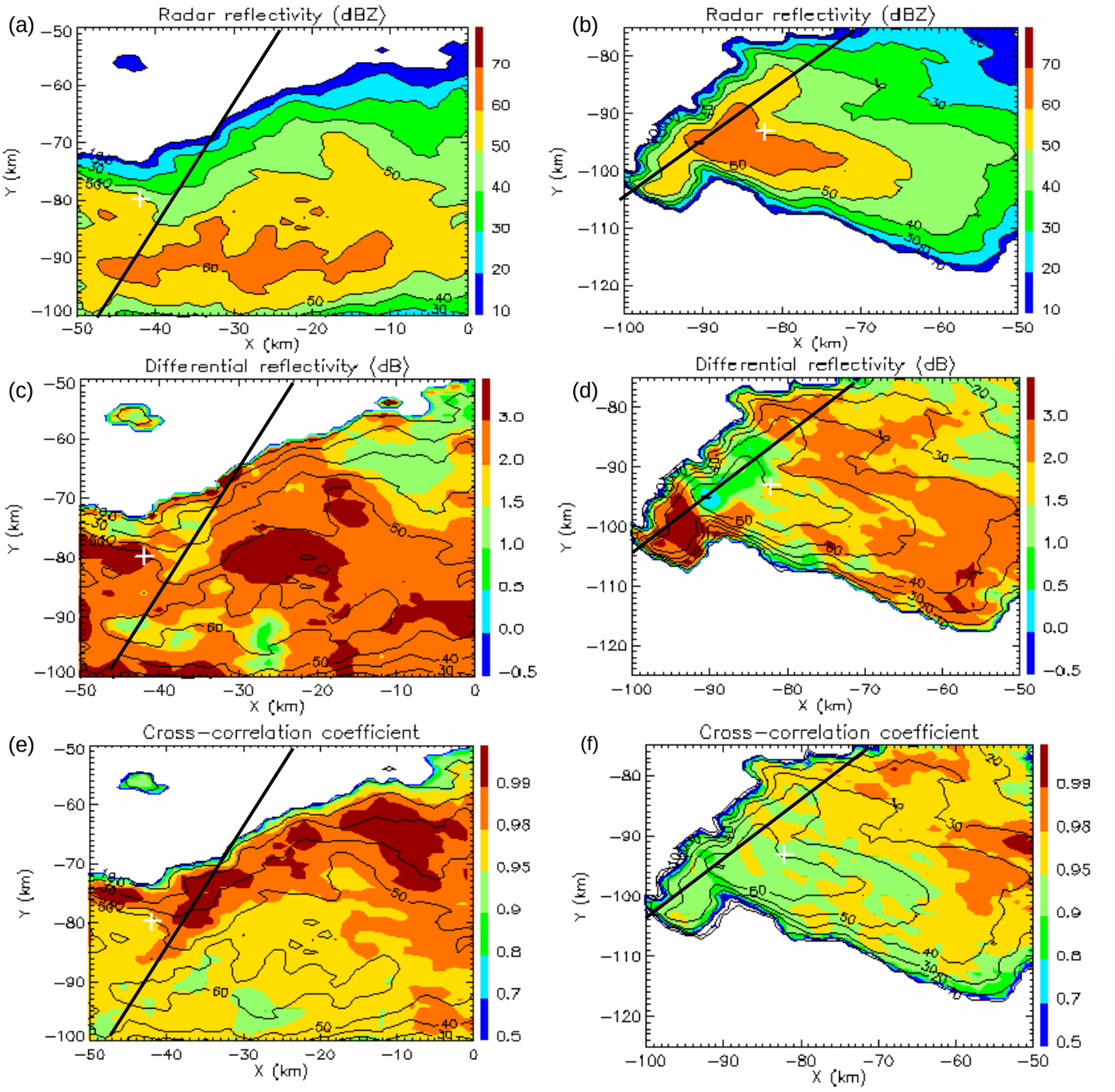

Figure 1. Plan Position Indicator (PPI) images created using IDL for the 0.5° elevation data. The PPI images for Z_H, Z_{DR}, and ρ_{HV} for the 1.00" hail report on 2 June 2004 at 2236 UTC are shown in (a), (c), and (e). The PPI images for the 1.75" hail report on 24 May 2004 at 0200 UTC are shown in (b), (d), and (f).

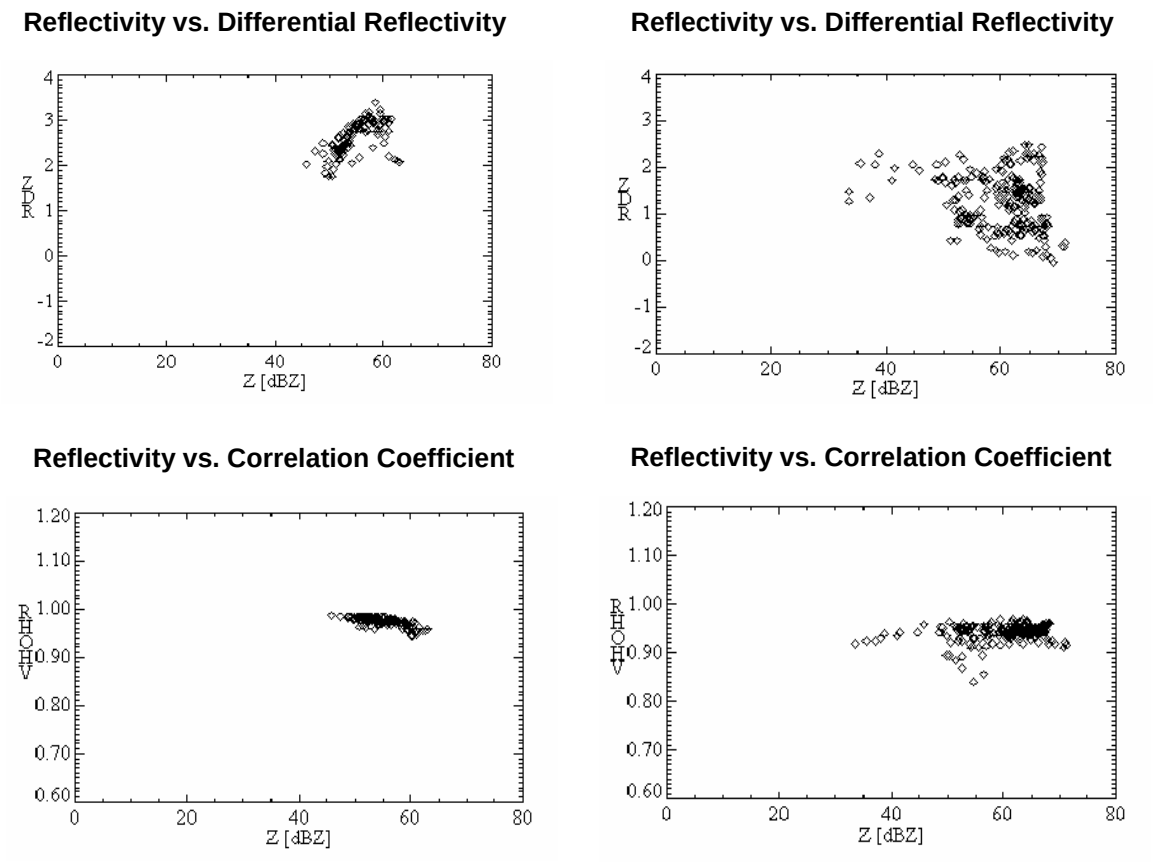

Figure 2. The two scatterplots in the left column are produced from the 2 June 2004 2236 UTC PPI image for 1.00" hail within a range of 99−104 km of KOUN and azimuth angles from 203−208°. The two scatterplots in the right column are produced from the 24 May 2004 0200 UTC PPI image for 1.75" hail within a range of 130−140 km of KOUN and azimuth angles from 203−208°.

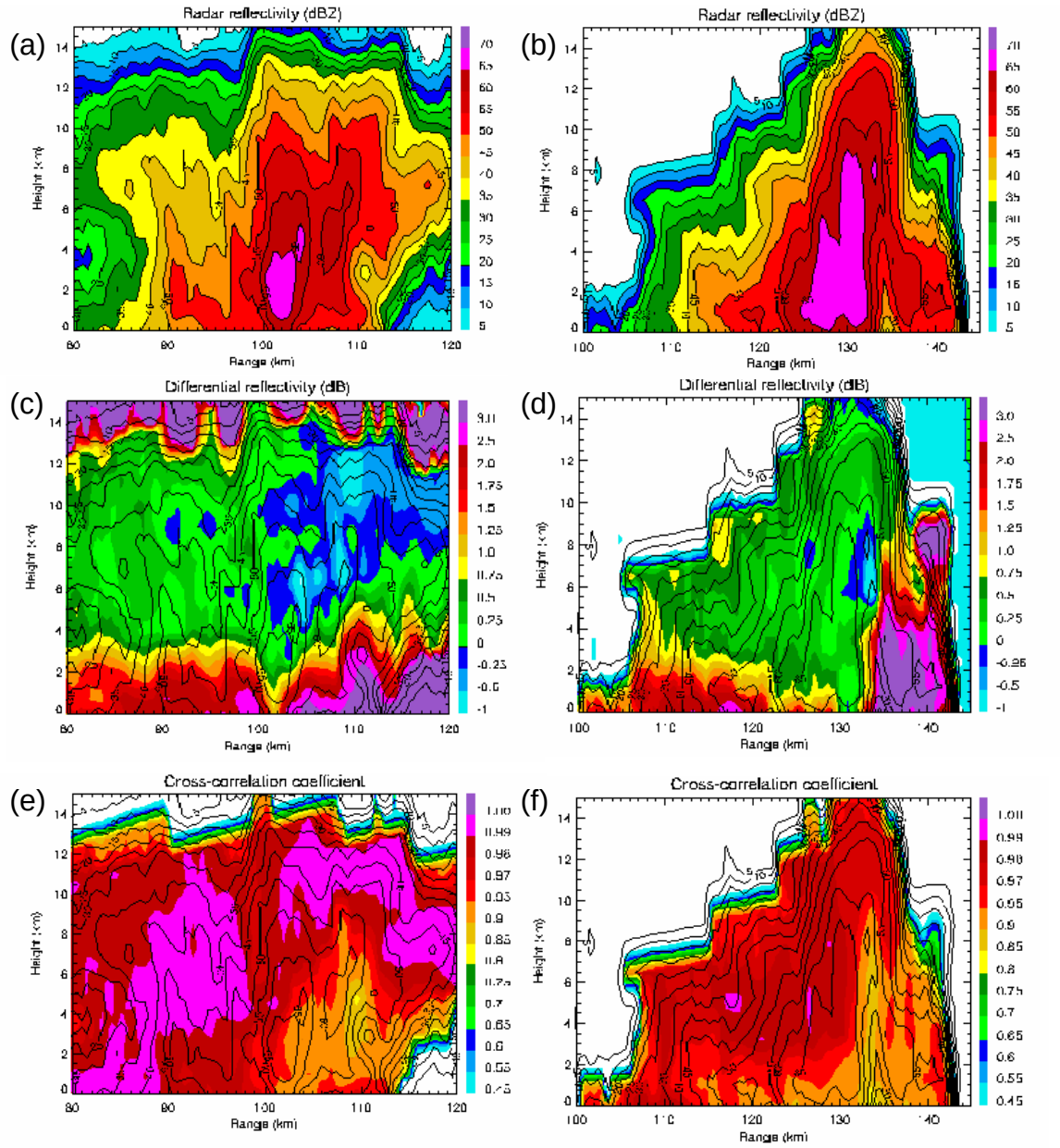

Figure 3. Range Height Indicator (RHI) images associated with the PPI images in Figure 1. The RHI images in the left column (a, c, and e) are the cuts through the 2 June 2004 2236 UTC PPI image for the 1.00" hail report at an azimuth of 206°. The RHI images in the right column (b, d, and f) are the cuts through the 24 May 2004 0200 UTC PPI image for the 1.75 hail report at an azimuth of 223°.

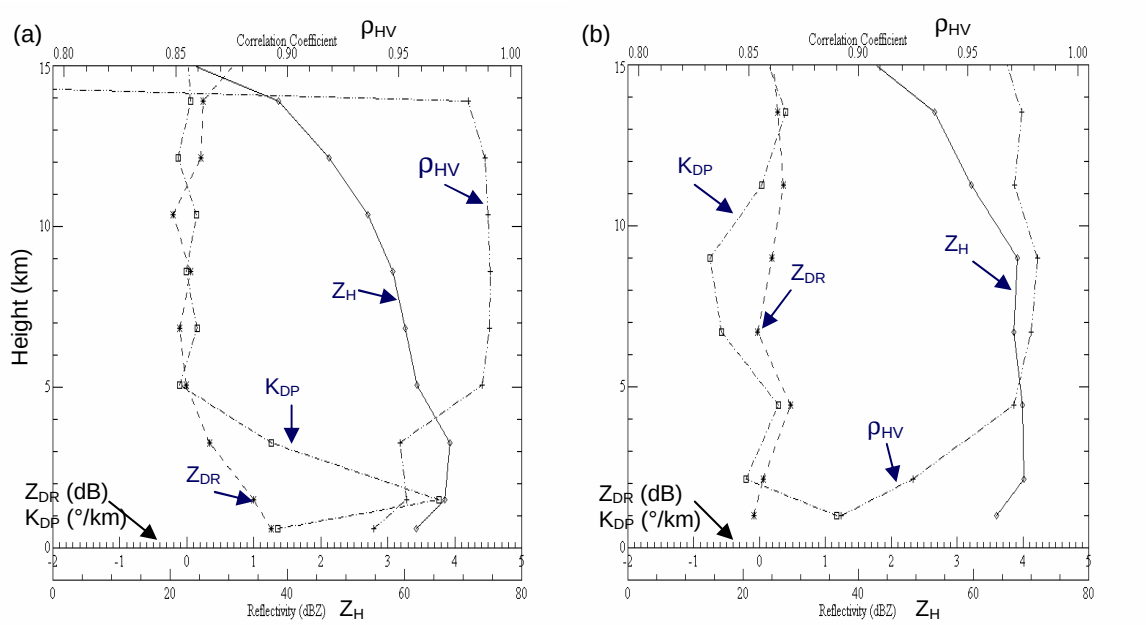

Figure 4. Vertical profiles of Z_H, Z_{DR}, ρ_{HV}, and K_{DP} on (a) 2 June 2004 at 2236 UTC 1.00" hail at 102 km from the radar and 206° azimuth and (b) 24 May 2004 on 0200 UTC 1.75" at 131 km from the radar and 223° azimuth.

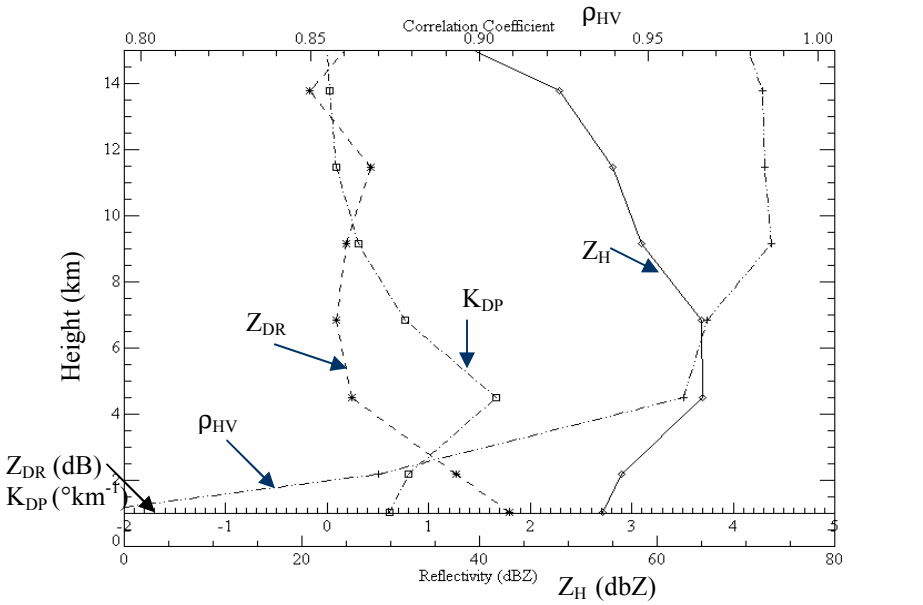

Figure 5. Vertical profile measured at 29 May 2004 2330 UTC for the 4.25" hail report at a range of 133 km from the radar and a 295° azimuth.

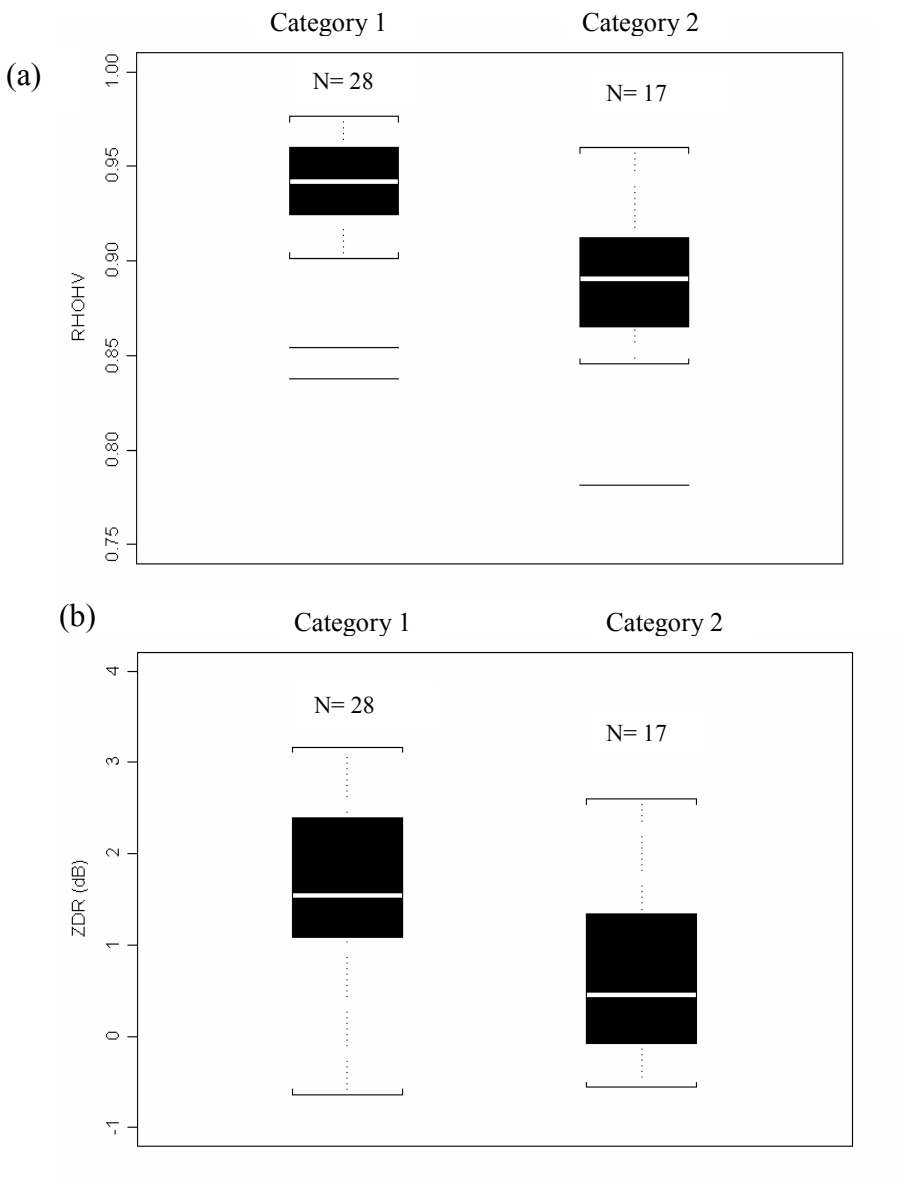

Figure 6. Box-and-whisker plots of (a) correlation coefficient and (b) differential reflectivity. Both plots contain 28 reports from category 1 and 17 reports from category 2. The white line represents the median of the data, the upper and lower values of the black boxes are the upper and lower quartiles, the brackets represent 1.5 times the inner quartile range, and the lines outside this range are the outliers of the data.

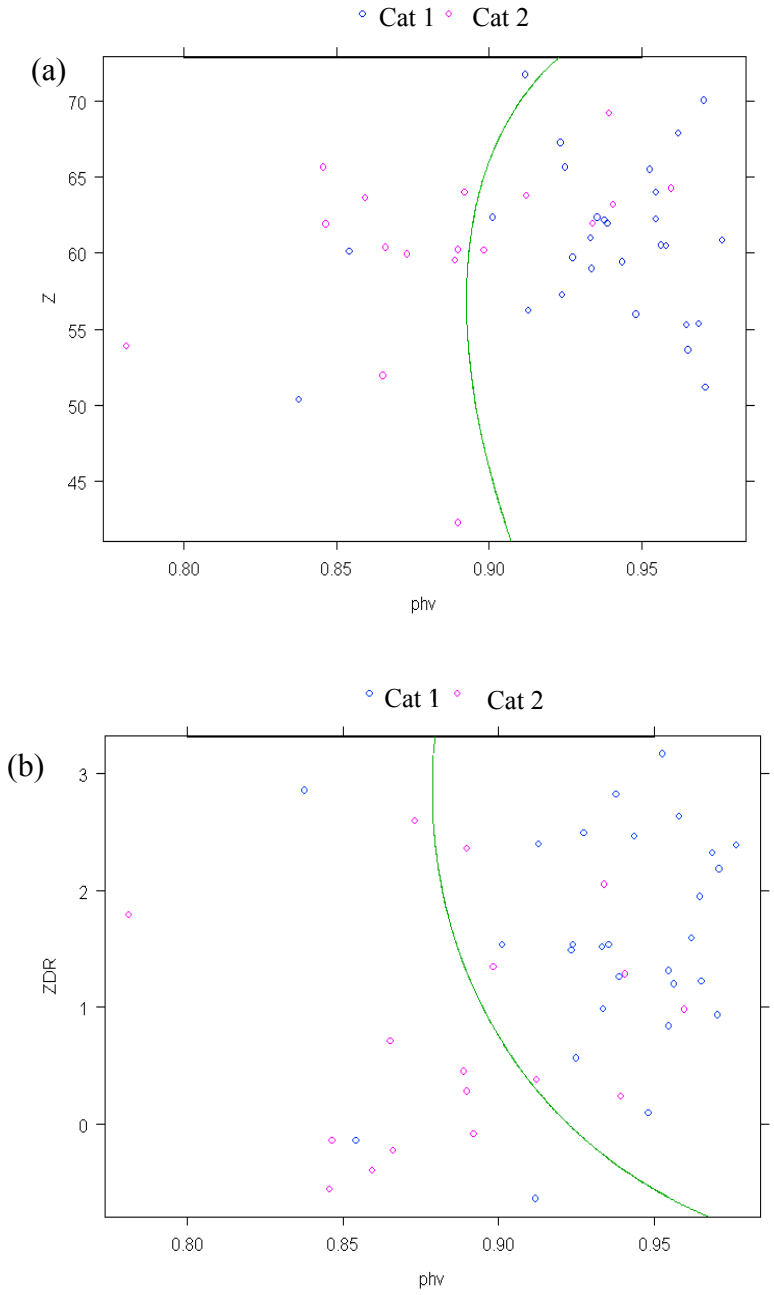

Figure 7. Discriminant analysis of (a) correlation coefficient and reflectivity and (b) correlation coefficient and differential reflectivity. Both plots correspond to 28 reports of category 1 hail and 17 reports of category 2 hail. The green line represents the quadratic discriminant function.